Far-infrared emission and Stark-cyclotron resonances in a quantum-cascade structure based on photon-assisted tunneling transition

Stéphane Blaser,* Michel Rochat, Mattias Beck, and Jérôme Faist†
Institute of Physics, University of Neuchâtel, CH-2000 Neuchâtel, Switzerland

Ursula Oesterle
Institute of Micro- and Optoelectronics, Swiss Federal Institute of Technology, CH-1015 Lausanne, Switzerland
(Received 14 September 1999; revised manuscript received 19 November 1999)

Intersubband electroluminescence has been investigated in a quantum cascade structure based on a photon-assisted tunneling transition designed for far-infrared emission. Transport measurements in the presence of a strong magnetic field perpendicular to the layers have been performed showing a strong increase of the lifetime increasing the magnetic field. In addition, Stark-cyclotron resonances were observed when the $n=0$ Landau level of an excited state is resonant with a Landau level of higher index of the lower state. Finally, good agreement was found between the electronic spectrum derived by the spectral characterization of the luminescence and the location of the Stark-cyclotron resonances in the transport data.

I. INTRODUCTION

Intersubband emission in superlattices has been suggested by the pioneering proposal by Kazarinov and Suris[1] more than two decades ago for both mid- (MIR) and far-infrared (FIR) wavelengths. Quantum cascade lasers based on such intersubband transitions have been successfully demonstrated in the midinfrared.[2] In contrast, the same quantum cascade technology in the far-infrared (FIR) have not yet been realized. Intersubband electroluminescence has been demonstrated at low temperature in the FIR in a periodic superlattice[3] and in a GaAs quantum cascade structure based on vertical transitions.[4,5] Broadband FIR emission has also been observed in a three-well quantum cascade structure based on diagonal transition.[6] Narrower electroluminescence has been reported recently by the same group.[7]

We show here intersubband electroluminescence in a quantum cascade structure based on a photon-assisted tunneling transition. Compared to the structure of Xu *et al.*,[6] which was based on depopulation of the middle-well-state through longitudinal optical phonon scattering, the emission occurs here between the ground state of one period and the excited state of the next period of our structure. The population inversion is maintained by the photon-assisted tunneling nature of the transition.[8] This diagonal transition allows the measure of the lifetime of the ground state by measuring the current flowing in the structure.

It is well known that a magnetic field (B) applied perpendicularly to the layers localizes the in-plane states into Landau levels.[9] This added localization offers the possibility of simulating a quantum box structure: the intersubband emission should occur between Landau levels instead of subbands. This in general will reduce the phase space for nonradiative scattering, increasing the lifetime of the state. A quantum cascade laser based on quantum boxes has already been the subject of numereous proposals.[10,11] Magnetic field enhanced terahertz intersubband emission has been observed experimentally by Ulrich *et al.*[12]

Indeed, at a fixed voltage, transport measurements in our structure in a perpendicular magnetic field show a strong current decrease with increasing field. We attribute this decrease of the current to an increase in intersubband lifetime as the transition occurs now between the well-defined Landau levels. In addition, maxima in the current vs magnetic field (I-B) characteristic are observed and attributed to Stark-cyclotron resonances (SCR). We are then able to identify the electronic spectrum with these magneto-transport measurements. Transport in superlattices in perpendicular electric and magnetic field have been the subject of many investigations[13–15] and these resonances have been first observed by Beltram *et al.*[16,17] in an undoped $GaAs/Al_xGa_{1-x}As$ superlattice structure. Then Liu *et al.*[18] obtained similar results in sequential resonant tunneling through Landau levels measurements.

II. SAMPLE STRUCTURE

Our structure was grown by molecular beam epitaxy on an n^+-doped GaAs substrate and consists of 50 periods. As shown in Fig. 1, one period of our three-well structure consists of three GaAs quantum wells of decreasing width separated by $Al_{0.15}Ga_{0.75}As$ tunnel barriers. The radiative transition is diagonal in real space and occurs via a 3.0 nm wide AlGaAs injection barrier between state $n=1'$ belonging to the third, narrower, GaAs quantum well of one period (width $=13.5$ nm) and state $n=3$ belonging to the first, broader, GaAs well of the following period (width$=18.5$ nm).

Because of the photon-assisted tunneling nature of the $n=1'$ to $n=3$ transition, the lifetime of the ground state of one period is much longer than the intersubband lifetimes of the other states.[8] So, in the bias voltage range studied, the ground state contains the majority of the electron population. The electron density in this state is therefore quasiconstant and the population inversion is then also maintained in a wide range of electric fields. Moreover, a measurement of the current flowing in the structure allows then to derive the lifetime of the upper state ($n=1'$) of the transition. Compared to vertical transitions, like reported in a previous

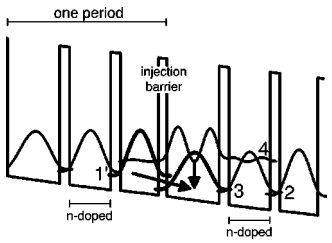

FIG. 1. Self-consistent computation of the energy band diagram of two periods of the structure under an average applied electric field of 5.3 kV/cm. Shown are the moduli squared of the relevant wave functions. The diagonal arrow corresponds to the radiative transition 1'-3 and the vertical one to the vertical transition 4-3 identified in the luminescence spectra (see text). The layer sequence of one period of the structure left to right and finishing with the injection barrier is 18.5/**3.5**/14.5/**3.5**/13.5/**3.0**. The thickness is in nanometers, and the thickness of the $Al_{0.15}Ga_{0.75}As$ layers is indicated in boldface.

paper,[4] the diagonal transition has a smaller oscillator strength and a broader linewidth due to the interface roughness; however it has the potential of a better lifetime ratio for population inversion.

The center quantum well of each period is doped with Si to minimize space-charge effects. The electronic sheet carrier density per period n_s induced by the doping was measured by capacitive measurements. The sample was etched to remove the n-doped GaAs layers above the active region and contacts were evaporated on it. The dependence of the capacity C on bias allows to determine the sheet density. Indeed the differential capacity can be written[19] as $C(V) = dQ/dV = (\varepsilon\varepsilon_0 e N_d/2)^{1/2} \cdot V^{-1/2}$. So the average density N_d as a function of the space charge distance W is $N_d(W) = [2/\varepsilon\varepsilon_0 e] \cdot [dV/d(1/C^2)]$, where ε is the dielectric constant and ε_0 the vacuum permittivity. We found for our sample (numbered as S1443) a value of $N_d = 2.95 \times 10^{15}$ cm^{-3} leading to an electronic sheet carrier density of $n_s = 1.67 \times 10^{10}$ cm^{-2}. This is about twice as large as the expected value $n_s = 0.87 \times 10^{10}$ cm^{-2} from the design.

III. OPTICAL MEASUREMENTS

A. Spectra

For optical characterization, the sample was processed into 420 μm$\times$420 μm mesas with Au/Ge ohmic contacts on top. The light was coupled out of the structure through an evaporated Ti/Au metal grating of 15 μm periodicity. The sample was mounted on the cold finger of a He flow cryostat. Bursts of 1.7 μs long current pulses at 2.1 μs intervals were injected into the device, providing an overall duty-cycle of 40% at 413 Hz, in order to match the frequency response of the bolometer detector while minimizing heating effects. The light was then collected by a wide numerical aperture gold coated parabolic off-axis mirror and sent through a Fourier transform infrared (FTIR) spectrometer on a helium-cooled Si bolometer detector. An optical calibration of the Si bolometer has been performed using a blackbody radiation source. A large difference between the electric and optical responsivity has been observed. Indeed the optical responsivity was found to be only 13% of the claimed electrical responsivity specified by the manufacturer.[20] A schematic drawing of the experimental set up is shown in Ref. 4.

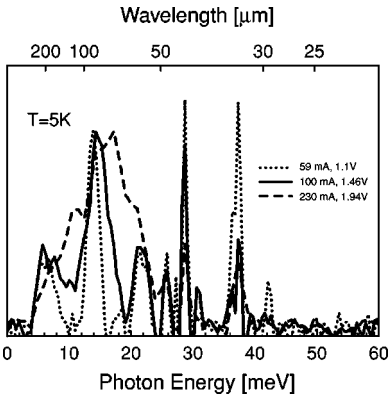

FIG. 2. Luminescence spectra of the emitted radiation for three different injected currents at $T = 5$ K.

Luminescence spectra at various bias voltages were obtained using the FTIR in step-scan mode, the signal being detected with a lock-in amplifier. A few representative spectra taken for increasing injected currents at $T = 5$ K are displayed in Fig. 2. They show that the luminescence spectrum consists at mainly three peaks. The first peak centered at a wavelength of $\lambda = 87$ μm is identified as the desired $n = 1'$ to $n = 3$ diagonal transition as its measured photon energy of 14.3 meV corresponds to the calculated value of the designed transition energy of 14.2 meV. The second peak is identified as the vertical transition between the $n=4$ and $n=3$ state in the 18.5 nm well; its measured photon energy of 28.7 meV corresponds exactly to the calculated value of this transition energy. The oscillator strength of the diagonal and vertical transitions are calculated as 1.2 and 14.8, respectively. The origin of the peak at $h\nu \sim 37$ meV, which was also observed in our previous structure, is attributed to a grating artifact. The ratio of the intensities of the peaks due to the $n = 1'$ to $n = 3$ diagonal transition and $n = 4$ to $n = 3$ vertical transition gives an electron temperature of $T = 40$ K.

The position of the 1'-3 transition as a function of applied bias is displayed in Fig. 3 along with the calculated values. The magnitude of the Stark tuning is significantly lower than

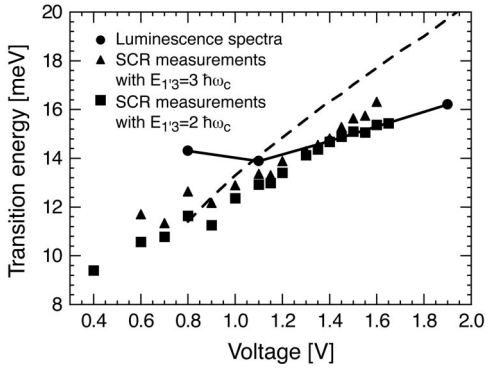

FIG. 3. Luminescence peaks energy vs voltage, which corresponds to the observed Stark-shift and transition energy obtained by SCR measurements (see further in the text) with $E_{1'3} = \delta n \cdot \hbar\omega_c$ for $\delta n = 2$ (squares) and 3 (triangles). The dashed curve represents the calculated Stark-shift.

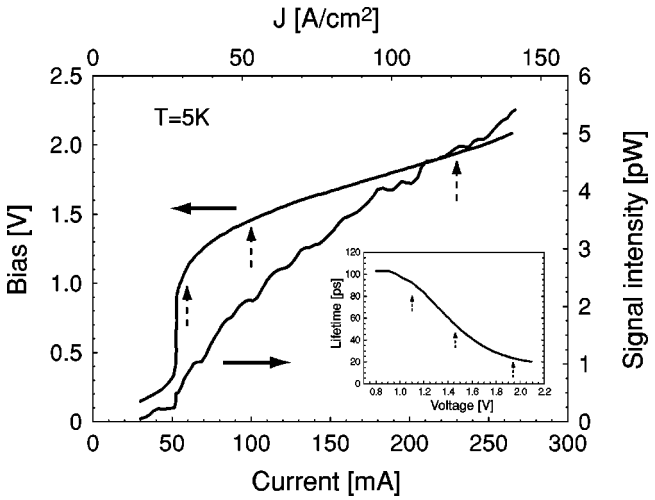

FIG. 4. Luminescence intensity and bias vs injected current at $T=5$ K. Inset: lifetime of the upper state of the transition vs voltage. The dashed vertical arrows indicate the position of the luminescence spectra of Fig. 2.

the calculated values. The origin of this discrepancy is not clear especially since the Stark-cyclotron resonances measurements (see further in the text) do not show such a strong discrepancy.

B. Lifetime with $B=0$

Figure 4 displays transport measurements such as voltage vs current (V-I) and light intensity vs current (L-I) curves, which were performed on the same device at $T=5$ K. In the V-I curve, one observes a region where negative differential resistance (NDR) occurs. This region was avoided in the electroluminescence spectra, because NDR is an indication for electrical instability of the device. As mentioned, one can, from these V-I curves, easily deduce the ground state lifetime τ_{nr} as a function of the voltage using the relation $\tau_{nr}=n_s q/j$, where n_s is the sheet density, q is the electronic charge, and j the current density. With the value for the sheet density measured by capacitive measurements, one obtains a lifetime which decreases between $\tau_{nr}=100$ ps at 0.8 V and $\tau_{nr}=20$ ps at 2 V, as shown in the inset of Fig. 4.

In such structures based on photon-assisted tunneling, a necessary condition for electrical stability is that the overall scattering rate of the state $n=3$ should increase with increasing electric field. But, due to the Stark effect, the transition energy $E_{1'3}$ increases with the applied electric field and thus the electron-electron w_{ee} and elastic $w_{elastic}$ scattering tend to decrease with increasing momentum exchange Δk, i.e., with increasing subband separation ($w_{ee}, w_{elastic} \sim 1/E_{1'3}$ and $\Delta k \sim \sqrt{E_{1'3}}$). To compensate the latter effect, the tunneling matrix element between the states $n=1'$ and $n=3$ should increase. In contrast to the work of Ref. 8, this tunneling matrix element is basically constant with applied electric field and therefore the structure is not electrically stable in the range of voltage 0.3 - 0.8 V. As we will see, the NDR can disappear with the application of a magnetic field on the structure.

From a $n=1'$ to $n=3$ optical matrix element of about 1.8 nm (for an injected current of 100 mA), we derive a radiative lifetime of 63 μs and a radiative efficiency $\eta_{rad}=\tau_{nr}/\tau_{rad} \sim 8.7\times10^{-7}$. The optical power P_{opt} is related to the injected current I by $P_{opt}=\eta_{coll}\eta_{rad}N_{per}I/q_0 h\nu$, where η_{coll} is the collection efficiency, N_{per} the number of periods and $h\nu$ the photon energy. If we take a collection efficiency of $\sim 1.3\times10^{-4}$ like in our previous paper (a value confirmed by new measurements on structures with vertical transition in GaAs and $In_xGa_{1-x}As$ wells[21]), we calculate an expected optical power of 9.6 pW. This is between 4 and 5 times larger than the optical power obtained in luminescence measurements.

This discrepancy could have several reasons. Because of the small energy difference with the $n=1'$ state, the population of the $n=2'$ ($E_{1'2'} \sim 3.7$ meV) and $n=3'$ ($E_{1'3'} \sim 7.1$ meV) could be increased if the electron temperature is high. So the lifetime of the $n=1'$ state should decrease. Moreover, the grating efficiency that involves in the collection efficiency could strongly depend on the processing. The matrix element of the transition could also be smaller than the calculated one.

IV. TRANSPORT MEASUREMENTS

A. Lifetime vs magnetic field

We investigated the behavior of the structures in a strong magnetic field. This field cannot be considered only as a perturbation. Indeed the magnitude of the cyclotron energy $\hbar\omega_c$, where $\omega_c=eB/m^*$, is about of the same or even larger magnitude as the transition energy $h\nu$ ($\hbar\omega_c \sim 17$ meV at 10 T). We measured V-I and I-B curves in a magnetic field perpendicular to the layers.

For these transport measurements, the sample was processed into 120 μm$\times$120 μm mesas with Au/Ge ohmic contacts on top. The samples were mounted on a special holder that allowed us to characterize them in a field perpendicular to the layers. The magnetic field with a maximum strength of 14 Tesla was produced by a superconducting magnet. V-I and I-B measurements were performed using a Keithley 2400. The sample temperature could be varied between 2 and 300 K using a needle flow control valve between helium bath and sample tube.

The scaling of the V-I curves with different mesa area has been verified. In particular, the V-I curves of the 120 $\times$120 μm^2 mesas without magnetic field are the same as the V-I curves on the 420$\times$420 μm^2 mesas made during the spectral measurements.

V-I curves are plotted at 2 K for zero, 7, and 12 Tesla in Fig. 5. They show clearly that, at a fixed voltage, the current decreases strongly with increasing magnetic field. This overall decrease is in good agreement with the picture in which the intersubband transitions occur between dispersionless Landau levels instead of subbands, efficiently quenching the non-radiative transitions.

In addition, the current range where NDR occurs shifts in current density and even disappears in the range of 2–4 and 5.5–10 Tesla. Figure 8 shows in gray areas the regions where NDR occurs for sample S1443 as a function of the magnetic field and voltage. The magnetic field seems to suppress the NDR in this particular range and then to stabilize the structure. In order to study the behavior of the current

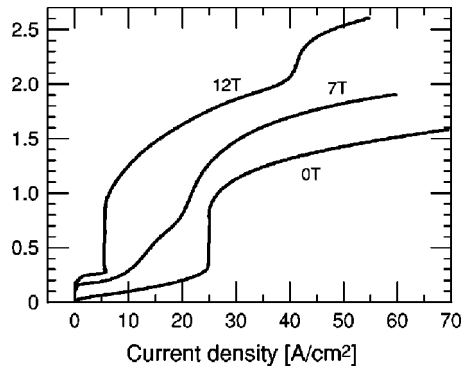

FIG. 5. Voltage vs injected current curves at zero, 7 and 12 Tesla at $T=2$ K. A NDR region occurs at zero and 12 Tesla, but not at 7 Tesla.

(and lifetime) in the structure as a function of the magnetic field, I-B curves were performed by setting the external voltage to a fixed value while ramping B between zero and maximum. It is now possible to plot the lifetime as a function of the magnetic field as shown in Fig. 6. As already mentioned, the lifetime is about 40–100 ps at zero field depending on the voltage. Depending on the applied voltage, one observes a substantial lifetime increase with the magnetic field up to about 400 ps, which is a factor of 4 compared to the value without magnetic field. This increase became important only above 6 T, where $\hbar\omega_c \sim 10.5$ meV, which is comparable to the transition energy of ~ 14 meV. It corresponds to the strong decrease of the current as a function of the magnetic field observed in the V-I curves. A lifetime increase or intersubband relaxation rate slowdown has already been observed[12] in quasi quantum dots[22] created also by magnetic confinement, and in a three-barrier, two-well heterostructure.[23] This effect holds promises for a FIR quantum cascade (QC) laser working by applying a magnetic field.

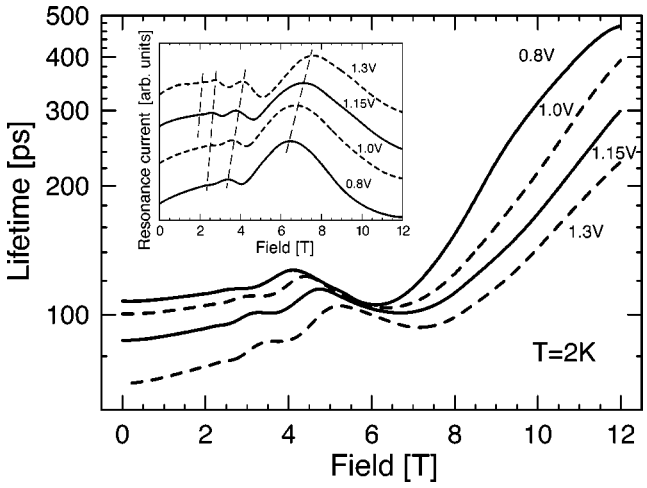

FIG. 6. Lifetime of the upper state of the transition vs applied magnetic field for different voltages at $T=2$ K. Inset: I-B curves with substracted background current (exponential fit used to better identify the resonance maxima) for the same voltages. The curves are vertically displaced for clarity. The dashed lines show the resonance maxima.

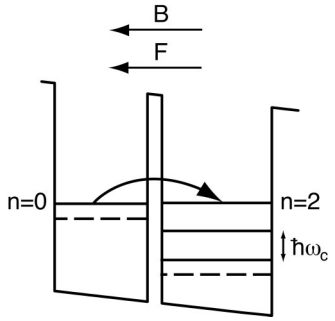

FIG. 7. Schematic representation of the Stark-cyclotron resonance (SCR) for a Landau-level index change $\delta n=2$.

The I-B curves show also maxima which we attribute to the Stark-cyclotron resonances. These resonances have previously been observed in superlattices.[16,17]

B. Stark-cyclotron resonances

When a strong external electric field F is applied perpendicularly to the layers of a superlattice, it destroys its minibands and localizes the electronic states along the growth axis forming a Wannier-Stark ladder separated in energy by eFd, where e is the electron charge and d is the superlattice period. As already mentioned, a magnetic field applied perpendicularly to the layers localizes the in-plane states into the well-known Landau levels.[9] In such systems, a resonance occurs due to elastic tunneling between Wannier-Stark-Landau (WSL) levels with nonequal quantum numbers on neighboring wells. There are so-called Stark-cyclotron resonances (SCR), which occur if the energies of the initial and final states coincide.[24]

One observes here that this phenomenon also arises in far-infrared (FIR) quantum cascade (QC) structures based on photon assisted tunneling[8] where the carrier transport is controlled by a diagonal transition between the ground state of one period of the structure and an excited state of the next one. In more general terms, it is expected to occur whenever transport across the structure is limited or controlled by the lifetime of a single excited state,[25] i.e. when the transport time across one period is much shorter than the electron lifetime of the upper transition state.[8] In such a case, the current will show maxima at magnetic fields corresponding to the

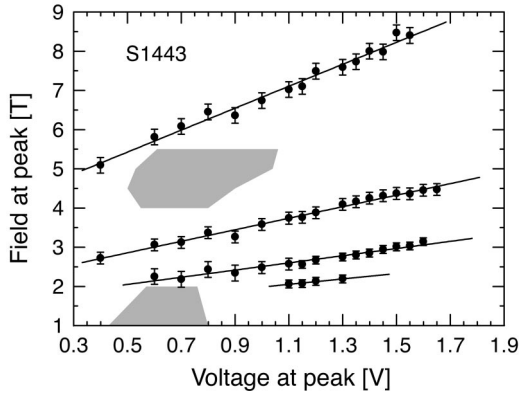

FIG. 8. Experimental (B_p, V_p) points at Stark-cyclotron resonance with the fits resumed in Table I for sample S1443. The gray areas correspond to the regions where NDR occur.

TABLE I. Results of linear fit for the data of Figs. 8 and 9. The SCR resonances are identified by computing the ratios of $a(1)/a(\delta n)$.

	S1443		S1351	
δn	$a[T/V]$	$a(1)/a(\delta n)$	$a\ [T/V]$	$a(1)/a(\delta n)$
1	2.8 ± 0.3	[1]	3.2 ± 0.4	[1]
2	1.5 ± 0.2	1.9 ± 0.2	1.6 ± 0.3	2.07 ± 0.3
3	0.9 ± 0.2	3.1 ± 0.3	1.1 ± 0.2	3.0 ± 0.3
4	0.7 ± 0.3	4.0 ± 0.5		

SCR condition $E_{1'3}=\delta n\hbar\omega_c$, where $\omega_c=eB/m^\star$ is the cyclotron frequency and δn is the Landau-level index change. Figure 7 sketches the SCR condition for a Landau-level index change $\delta n=2$. It is important to specify that coherent tunneling between WSL levels with different Landau indices is forbidden. Then the only tunneling allowed is elastic scattering.

The resonances are clearly resolved in the I-B curves (see Fig. 6). They are superimposed on a slowly varying background. The origin of this background is probably related to a slowly varying change in the nonradiative scattering due to the localization coming from the magnetic field. For a better identification of the resonance maxima, we fitted these raw data with an exponential fit, which was subsequently subtracted. The inset of Fig. 6 diplays such curves with subtracted background current showing the resonances in I-B characteristics for four bias voltages $V_{bias}=0.8$, 1.0, 1.15, and 1.3 V.

To confirm SCR with our experimental resonances, we extracted the positions of magnetic field peaks (B_p) for several different external voltages (V_p) from I-B curves. In Fig. 8, one can see the (B_p, V_p) points plotted for the sample measured. According to the above equation, a plot of the magnetic field values for which a SCR occurred as a function of applied voltage should align on straight lines. Experimental points clearly align along lines for the interval between 0.6 and about 1.6 V. The slopes of these lines are inversely proportional to the Landau-level index change δn, since $B_p\alpha V_p/\delta n$. Table I summarizes the values of the fitted slopes. Looking at the ratios of the slopes to the first one (at higher field), the SCR conditions for transitions with $\delta n=1$, 2, 3, and 4 are perfectly identified. In contrast to earlier papers of Beltram *et al.*,[16,17] we observed more easily the transitions with Landau-level index change $\delta n=1$, but experienced more difficulty in measuring those with $\delta n=4$. As Fig. 9 and the two last columns of the Table I show, we obtained similar results on an other, heavily doped, sample (S1351: $n_s=7.06\times10^{10}$ cm^{-2} measured by capacitive measurements), except for $\delta n=4$.

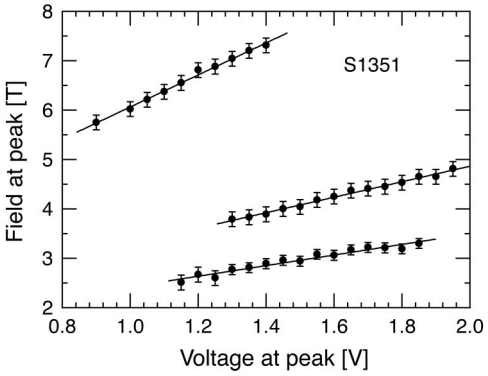

FIG. 9. Experimental (B_p,V_p) points at Stark-cyclotron resonance with the fits resumed in Table I for sample S1351.

C. Comparison spectra-transport measurements

We can derive the transition energy with the SCR resonances using the fact that $E_{1'3}=\delta n\cdot\hbar\omega_c$. Figure 3 shows the comparison between the transition energy vs voltage corresponding to the spectra and that obtained by SCR with $\delta n=2$ and 3, which corresponds to the resonances occuring at a relatively small magnetic field. The measurements of SCR show good agreement with the calculated Stark-shift (dashed curve in Fig. 3) given the uncertainty in the calculation. Finally, this figure shows the reasonable agreement of the electronic spectrum and the location of the SCR in the transport measurements.

V. CONCLUSION

In summary, we have shown far-infrared intersubband electroluminescence in a photon-assisted tunneling transition. Transport measurements have allowed to determine the relaxation lifetime of the upper state of the transition. A strong magnetic field was applied on the structure to study the behavior of the V-I characteristic. We observed a strong increase of the lifetime up to 400 ps corresponding to a factor of 4 compared to the value without applied magnetic field. The I-B curves showed maxima corresponding to the the Stark-cyclotron resonances. Computing the ratios of the slopes obtained in the (B_p, V_p) plot, very good agreement is found with the SCR condition and the transitions involving Landau-level index change $\delta n=1$, 2, 3, and 4 are clearly identified. The electronic spectrum is in reasonable agreement with the location of the SCR in transport measurements.

ACKNOWLEDGMENTS

We would like to thank Laurent Diehl for his help with transport measurements and Daniel Hofstetter for his careful reading of the manuscript. This work was supported by the Swiss National Science Foundation.

*Electronic address: Stephane.Blaser@iph.unine.ch
†Electronic address: Jerome.Faist@iph.unine.ch

[1] R.F. Kazarinov and R.A. Suris, Fiz. Tekh. Poluprovodn. **5**, 797 (1971) [Sov. Phys. Semicond. **5**, 707 (1971)].
[2] J. Faist, F. Capasso, D.L. Sivco, C. Sirtori, A.L. Hutchinson, and A.Y. Cho, Science **264**, 553 (1994).
[3] M. Helm, P. England, E. Colas, F. DeRosa, and S.J. Allen, Jr., Phys. Rev. Lett. **63**, 74 (1989).
[4] M. Rochat, J. Faist, M. Beck, U. Oesterle, and M. Ilegems, Appl. Phys. Lett. **73**, 3724 (1998).
[5] J. Ulrich, R. Zobl, N. F. K. Unterrainer, G. Strasser, and E. Gornik, Physics B **272**, 216 (1999).
[6] B. Xu, Q. Hu, and M.R. Melloch, Appl. Phys. Lett. **71**, 440 (1997).

[7] B.S. Williams, B. Xu, Q. Hu, and M.R. Melloch, Appl. Phys. Lett. **75**, 2927 (1999).
[8] J. Faist, F. Capasso, C. Sirtori, D.L. Sivco, A.L. Hutchinson, and A.Y. Cho, Nature (London) **387**, 777 (1997).
[9] L. Landau and E. Lifchitz, *Mécanique Quantique, Théorie Non Relativiste* (Editions Mir, Moscou, 1967), p. 496.
[10] C.F. Hsu, J.S. O, P.S. Zory, and D. Botez, Proc. SPIE, **3001**, 271 (1997).
[11] S.J. Lee and J.B. Khurgin, Appl. Phys. Lett. **69**, 1038 (1996).
[12] J. Ulrich, K. Unterrainer, G. Strasser, and E. Gornik, Appl. Phys. Lett. **76**, 19 (2000).
[13] Y. Lyanda-Geller and J.-P. Leburton, Phys. Rev. B **52**, 2779 (1995).
[14] R. Ferreira, Phys. Rev. B **43**, 9336 (1991).
[15] Yu. B. Lyanda-Geller and J.-P. Leburton, Solid State Commun. **106**, 31 (1998).
[16] L. Canali, M. Lazzarino, L. Sorba, and F. Beltram, Phys. Rev. Lett. **76**, 3618 (1996).
[17] L. Canali, F. Beltram, M. Lazzarino, and L. Sorba, Superlattices Microstruct. **22**, 155 (1997).
[18] J. Liu, E. Gornik, S. Xu, and H. Zheng, Semicond. Sci. Technol. **12**, 1422 (1997).
[19] H. Mathieu, *Physique des Semiconducteurs et des Composants Électroniques* (Masson, Paris, 1998), p. 254.
[20] The measured intensities in our previous paper (Ref. 4) should be multiplied by 7 to be consistent with this new calibration.
[21] M. Rochat, M. Beck, J. Faist, U. Oesterle, and M. Ilegems (unpublished).
[22] B.N. Murdin, A.R. Hollingworth, M. Kamal-Saadi, R.T. Kotitschke, C.M. Ciesla, C.R. Pidgeon, P.C. Findlay, H.P.M. Pellemans, C.J.G.M. Langerak, A.C. Rowe, R.A. Stradling, and E. Gornik, Phys. Rev. B **59**, 7817 (1999).
[23] Y. Ji, Y. Chen, K. Luo, H. Zheng, Y. Li, C. Li, W. Cheng, and F. Yang, Appl. Phys. Lett. **72**, 3309 (1998).
[24] F. Claro, M. Pacheco, and Z. Barticevic, Phys. Rev. Lett. **64**, 3058 (1990).
[25] C. Sirtori, F. Capasso, J. Faist, A.L. Hutchinson, D.L. Sivco, and A.Y. Cho, IEEE J. Quantum Electron. **34**, 1722 (1998).